



POLITECNICO DI TORINO
Repository ISTITUZIONALE

Development of a Clutch Assisted
Engine Start

Original

Development of a Clutch Assisted Engine Start / Brunetti, Gianmarco. - (2014).

Availability:

This version is available at: 11583/2543152 since:

Publisher:

Politecnico di Torino

Published

DOI:10.6092/polito/porto/2543152

Terms of use:

Altro tipo di accesso

This article is made available under terms and conditions as specified in the corresponding bibliographic description in the repository

Publisher copyright

(Article begins on next page)

Capitolo 4

Clutch Assisted Start

Cranking the engine via clutch uses vehicle inertia to ramp up engine speed. Though, by transferring its kinetic energy, vehicle decelerates more. In subjective assessments, drivability¹ is rated by evaluating the perception of the acceleration of the vehicle during pre-defined conditions.

The vehicle acceleration \dot{v}_v results from both the drive torque at the wheels T_w and the actual road load forces F_{res} , including road inclination or aerodynamic drag. The drive torque on the wheels can be controlled through the amount of torque exchanged through the clutch.

Therefore, an opportune control of the clutch closure defines the amount of clutch input force satisfying main requirement of achieving engine crank both smoothly, not to affect drivability, and fast enough not to increase delay in providing propulsion torque when driver accelerate. Automatic clutch system, both hydraulically and electrically automated as in automatic transmission and automated ones² are required in order to implement such strategies. Automation of transmissions, in general, paves the way towards introduction of such logic.

Clutch engages smoothly if the vehicle acceleration has a continuous and preferably non-negative derivative when clutch reaches touch-point and starts transferring torque³. Though, excessive slipping of the clutch should be prevented in order to minimize wear and heat buildup.

Engaging the clutch too fast, in fact, results in abrupt jerking of the vehicle, tire slip and torsional oscillation of the drive-line, all of which make for an uncomfortable

¹The project refers to the longitudinal driver-vehicle interaction. Moreover, over this project, the perception of longitudinal acceleration will be evaluated to rate drivability.

²Automatic transmission refer to systems with torque converter, dual-clutch-transmission (DCT). Automated transmission refer to automated manual transmissions.

³Clutch kiss-point.

experience for the driver. Therefore, the design a clutch assisted start logic must fulfill the main requirements as:

- Minimizing the clutch lock-up time;
- Preventing jerking;
- Minimizing the energy dissipated during the slipping phase;
- Ensuring a good drivability of the vehicle.

Though, as these requirements are somehow conflicting, an opportune trade-off must be found.

4.1 Development of clutch control

4.1.1 Predictive reduced model

The modeling, set up in AMESim through specific blocks as in Figure 3.1, provides the computation of the dynamics equations of the system. For the sake of simplicity, a reduced mathematical model of the powertrain is presented and it is representative of AMESim model. Considering the equations that govern the powertrain behavior, the torque transferred through the clutch, the only variable of the system that can be controlled⁴, can be quantified. For the purpose of describing the process, a simplified engine system can be described as:

$$J_e \cdot \dot{\omega}_e = T_e - T_f - T_c \quad (4.1)$$

with J_e engine inertia (including flywheel), $\dot{\omega}_e$ engine angular acceleration, T_e torque delivered by the engine, T_f engine friction torque, T_c torque through the clutch.

The torque delivered from the clutch to the wheels and from wheels to the vehicle, as already quantified, can be expressed through the following relationship:

$$\begin{cases} T_w = T_c \cdot i_{FD} \cdot i_g - J_d \dot{\omega}_w \\ m_{vw} \cdot \dot{v} = \frac{T_w}{R_x} - F_{res} \end{cases} \quad (4.2)$$

Combining the two equations into one:

$$m_{vw} \cdot \dot{v} = \frac{T_c}{R_w} \cdot i_{FD} \cdot i_g - \frac{J_d}{R_w} \cdot \dot{\omega}_w - F_{res} \quad (4.3)$$

Recalling the definition of m_{vw} and J_d , then 4.3 can be written as:

⁴As a matter of facts, the clutch torque T_c depends directly on the clutch slave cylinder position

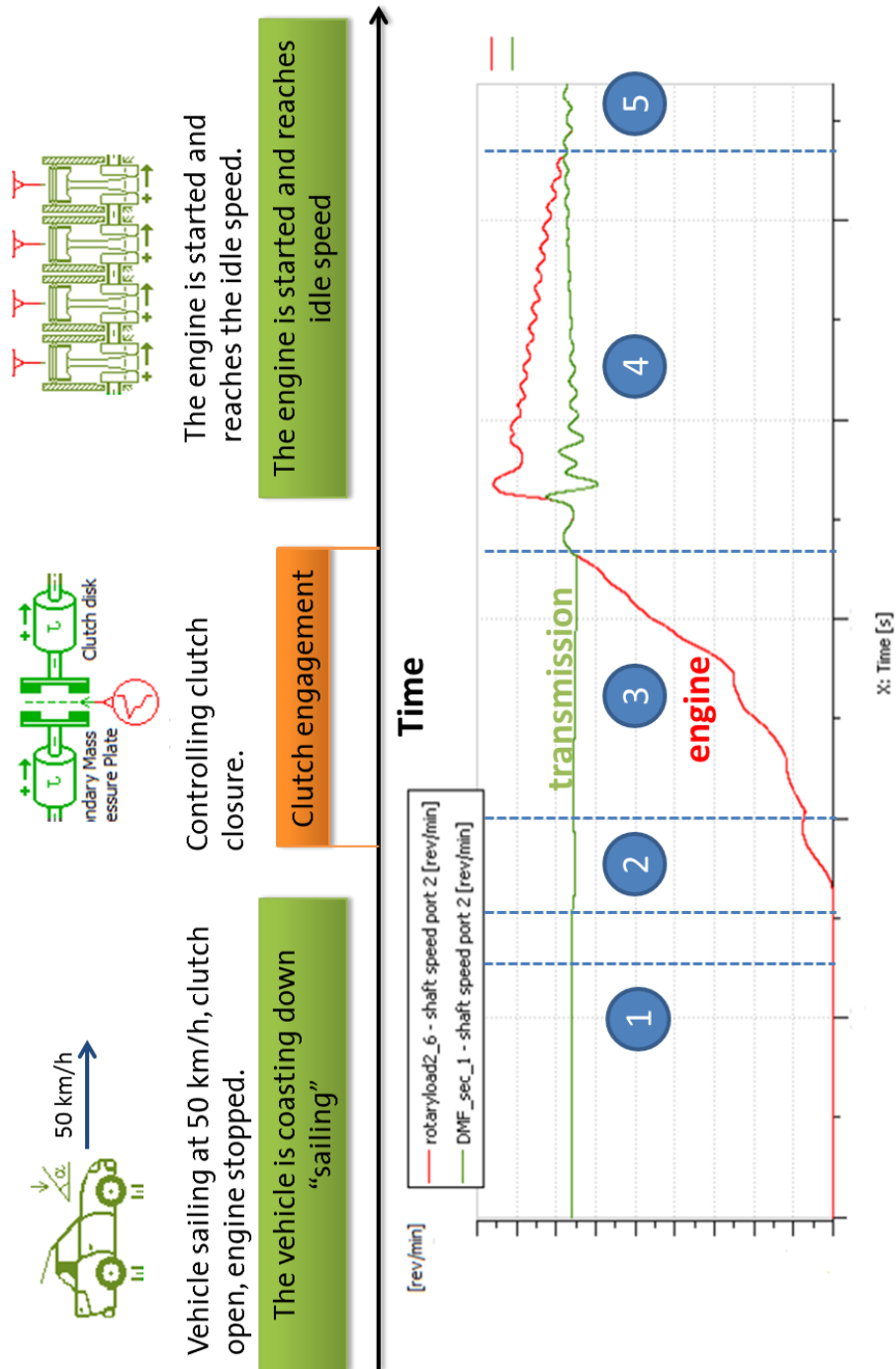


Figura 4.1: Basic explanation of clutch assisted start operation at tip-in.

$$\left(m_v + \frac{J_w}{R_w^2} + \frac{J_{gin}}{R_w^2} \cdot i_g^2 \cdot i_{FD}^2 + \frac{J_{diff}}{R_w^2} \right) \cdot \dot{v}_v = \frac{T_c}{R_w} \cdot i_{FD} \cdot i_g - \frac{J_d}{R_w} \cdot \dot{\omega}_w - F_{res} \quad (4.4)$$

Where the elements multiplying the vehicle acceleration \dot{v}_v can be considered as a lumped vehicle mass m_{vwt} (vehicle, wheels, transmission). And therefore:

$$m_{vwt} \cdot \dot{v}_v = \frac{T_c}{R_w} \cdot i_{FD} \cdot i_g - F_{res} \quad (4.5)$$

Finally, considering the equations governing the two sides of the clutch the system can be expressed as follows:

$$\begin{cases} J_e \cdot \dot{\omega}_e = T_e - T_f - T_c & \text{Engine side} \\ m_{vwt} \cdot \dot{v}_v = \frac{T_c}{R_w} \cdot i_{FD} \cdot i_g - F_{res} & \text{Drive-line side} \end{cases} \quad (4.6)$$

4.1.2 Main clutch operation

During clutch assisted start, vehicle operates in 3 different condition:

- **Sailing:** engine is disengaged from drive-line, vehicle is rolling;
- **Full Engagement:** engine is coupled to the drive-line, either delivering torque to the vehicle or being driven;
- **Clutch assisted engine crank:** engine is revved up from auto-stop⁵ through clutch engagement. The clutch, via slippage, transfers a certain amount of torque from the vehicle inertia to the engine, making the vehicle to decelerate unintendedly.

Sailing During Sailing, the engine is disengaged from the drive-line and therefore $T_c = 0$. Then, the deceleration of the vehicle is only due to external resistive forces.

$$\begin{aligned} m_{vwt} \cdot \dot{v}_v &= -F_{res} \\ \dot{v}_v &= -\frac{F_{res}}{m_{vwt}} \end{aligned} \quad (4.7)$$

⁵The Autostop is a fuel saving feature of Stop & Start vehicles, which causes the gas engine to shut-off during idling, as perhaps when the vehicle comes to a stop, at key-on.

Full engagement The clutch is in sticking condition (lock up) and the engine torque T_e , if present, can be delivered to accelerate the vehicle. The torque through the clutch (T_c) is the total torque exchanged between the engine side and the transmission side. This reduces the system into one equation.

$$m_{vwt} \cdot \dot{v}_v = \frac{1}{R_w} (T_e - T_f - J_e \cdot \dot{\omega}_e) \cdot i_{FD} \cdot i_g - F_{res} \quad (4.8)$$

Since the engine inertia is added to the system, a total lumped mass m_{tot} can be defined. It represents a fictitious translating mass that depends on the actual vehicle mass and on the engine and transmission rotational components inertia, affected, from the vehicle point of view, by the transmission ratios.

$$m_{tot} = m_v + \frac{J_w}{R_w^2} + \frac{J_{Diff}}{R_w^2} + \frac{J_{gout}}{R_w^2} \cdot i_{FD}^2 + \frac{J_{gin}}{R_w^2} \cdot i_g^2 \cdot i_{FD}^2 + \frac{J_e}{R_w^2} \cdot i_{FD}^2 \cdot i_g^2 \quad (4.9)$$

Therefore the acceleration of the vehicle can be evaluated from:

$$\dot{v}_v = \frac{1}{m_{tot}} \left[\left(\frac{T_e}{R_w} - \frac{T_f}{R_w} \right) \cdot i_{FD} \cdot i_g - F_{res} \right] \quad (4.10)$$

If there is no engine torque ($T_e = 0$), the engine is driven by the vehicle inertia and the fuel is cut off. In this condition it is clear that the vehicle acceleration (actually deceleration) depends on engine friction T_f , (which is a function of engine velocity) reflected to the vehicle through the transmission ratios, and on the lumped translating mass (high at low gears, and low at high gears). The clutch torque during the sticking phase can be found and it is given by:

$$T_c = \frac{m_{vwt}}{m_{tot}} \cdot \left[T_e - T_f - \frac{F_{res}}{i_{FD} \cdot i_g} \cdot R_w \cdot \left(\frac{m_{tot}}{m_{vwt}} - 1 \right) \right] \quad (4.11)$$

It is useful to recall that the sticking of the clutch sustains as long as the torque transmitted through the clutch remains below the maximum transmissible torque T_{cmax} .

Clutch assisted engine crank As the clutch starts the engagement phase, its two sides go into slipping condition and their relative velocity changes in time. As a matter of fact, the transmission side decelerates, while the engine crankshaft accelerates. Such phases is concluded as the two velocities become equal and the system enters in full engagement condition. The amount of torque delivered through the clutch determines the overall behavior of both

vehicle and engine. Optimizing drivability of the vehicle during clutch assisted start requires, therefore, calibration of clutch torque transferred over time.

The accelerations of the vehicle and of the engine are in this case different and they can be expressed as a function of the torque transmitted through the clutch.

$$\begin{cases} \dot{v}_v = \frac{1}{m_{vwt}} \cdot \left(\frac{T_c}{R_w} \cdot i_{FD} \cdot i_g - F_{res} \right) & \text{Vehicle acceleration} \\ \dot{\omega}_e = \frac{T_e - T_f - T_c}{J_e} & \text{Engine acceleration} \end{cases} \quad (4.12)$$

where T_c is the clutch torque as 3.14.

The clutch torque command expresses the amount of torque exchanged through the clutch, i.e. the value of T_c . Should an estimation of F_{res} be available, giving a desired vehicle acceleration profile, the torque through the clutch can be easily controlled from the first equation. Though, 4.11 does not take into account the effect of engine dynamic. Then, if the engine is not delivering any torque ($T_e = 0$) during all the starting maneuver, the vehicle deceleration required can be expressed as a function of engine acceleration and engine frictions:

$$\dot{v}_v = \frac{1}{m_{vwt}} \cdot \left[\left(-\frac{J_e \dot{\omega}_e}{R_w} - \frac{T_f}{R_w} \right) \cdot i_{FD} \cdot i_g - F_{res} \right] \quad (4.13)$$

Since T_f is known for a wide range of operating conditions from experimental maps, the desired engine angular acceleration $\dot{\omega}_e$ could be a useful parameter for controlling the vehicle deceleration and the resulting torque required through the clutch. In other words, by setting the desired final value of engine speed $\omega_{e\,fin}$ and crank time t_{start} , means to establish $\dot{\omega}_e$. The vehicle acceleration is computed from the above equation and the torque command can be derived from it.

4.1.3 Torque control

Clutch control must ensure a fast control of clutch slippage and driven disk acceleration over closure. An optimal control state feedback command the difference between the two speeds and the energy dissipated during the engagement. It is based on a Linear Quadratic (LQ) control theory. The control design problem is formulated as a finite time optimal control problem with initial time constraints (zero initial force) and final time constraints (the two speeds must be equal at the lock-up). Figura4.2 reports the normal force profile for LQ controller.

Simulation runs show that such force command profile results in less severe vehicle deceleration.

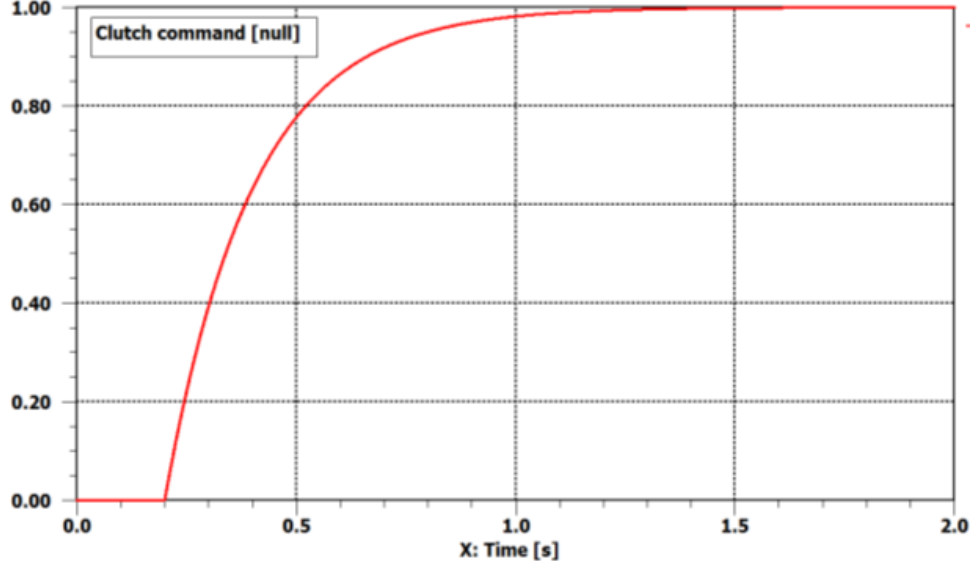


Figura 4.2: Command force profile for LQ controller.

4.1.4 Simulation results

The clutch control logic, then, has been implemented into the model developed in AMESim in Chapter 3, which provide all dynamic variables calculation.

Initial condition for a Clutch Assisted Start maneuver are:

- Vehicle coasting at a given initial velocity with the appropriate gear engaged.
- Clutch fully disengaged.
- Engine off (initial velocity 0).

The vehicle rolls due its inertia, then the clutch command imposes the amount of torque exchanged through the clutch. The clutch command was the one established from LQ controller, as already described. The engine starts and the vehicle consequently decelerates until full engagement is achieved. Gear influence the deceleration of the vehicle when performing clutch assisted start as 4.11. The only control parameter of the vehicle deceleration during clutch assisted start is the clutch torque T_c which is directly depending on the clutch slave cylinder position.

The major steps of clutch assisted start are deployed:

1. Vehicle sailing, engine off and clutch fully disengaged

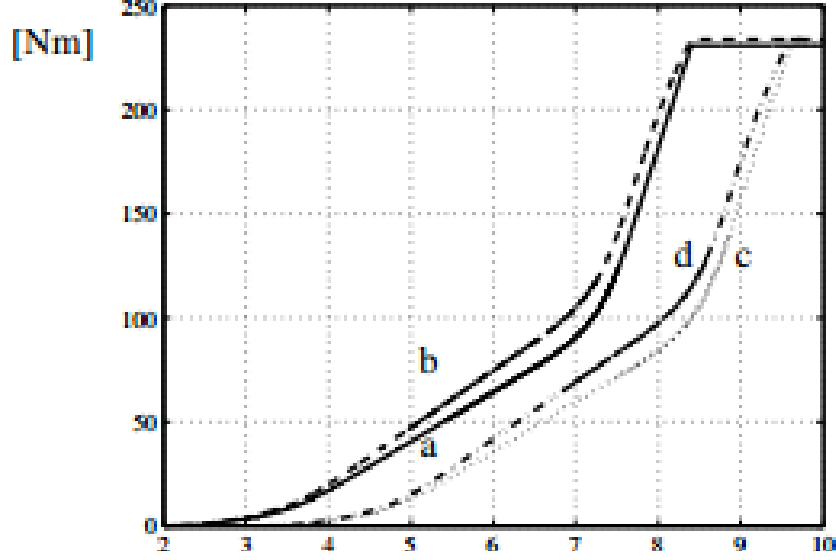


Figura 4.3: Torque transmitted T_c vs. throwout clutch position: (a, c) nominal characteristic, (b, d) characteristic: concave, (a,b) no wear, (c, d) in the presence of wear.(20)

2. Engine cranking, vehicle decelerating and clutch in slipping phase
3. Powertrain stabilizing phase due to DMF elastic parts, clutch fully engaged
4. Driveline engaging, engine either is powering the vehicle or is motored by the driveline

From the drivability point of view it is more useful to point out the resulting vehicle acceleration. In Figura4.4 the velocity and acceleration of the vehicle are presented. It can be noticed that in the first stage the vehicle is sailing and its velocity is slightly dropping due to aerodynamic drag. When the clutch engages and the engine starts, the deceleration increases until the end of clutch slipping phase. Vehicle drive-line might oscillate due to elasticity of DMF and tires, a phenomenon defined as *âjerkingâ*. Finally the engine is fully coupled with the transmission. The engine is ready to propel the vehicle.

4.2 Optimization of clutch control

Drivability is usually subjected to human perception, feeling. Therefore it cannot be directly derived from objective measures. The only way for an objective assessment and quality control of drivability based on human experience are

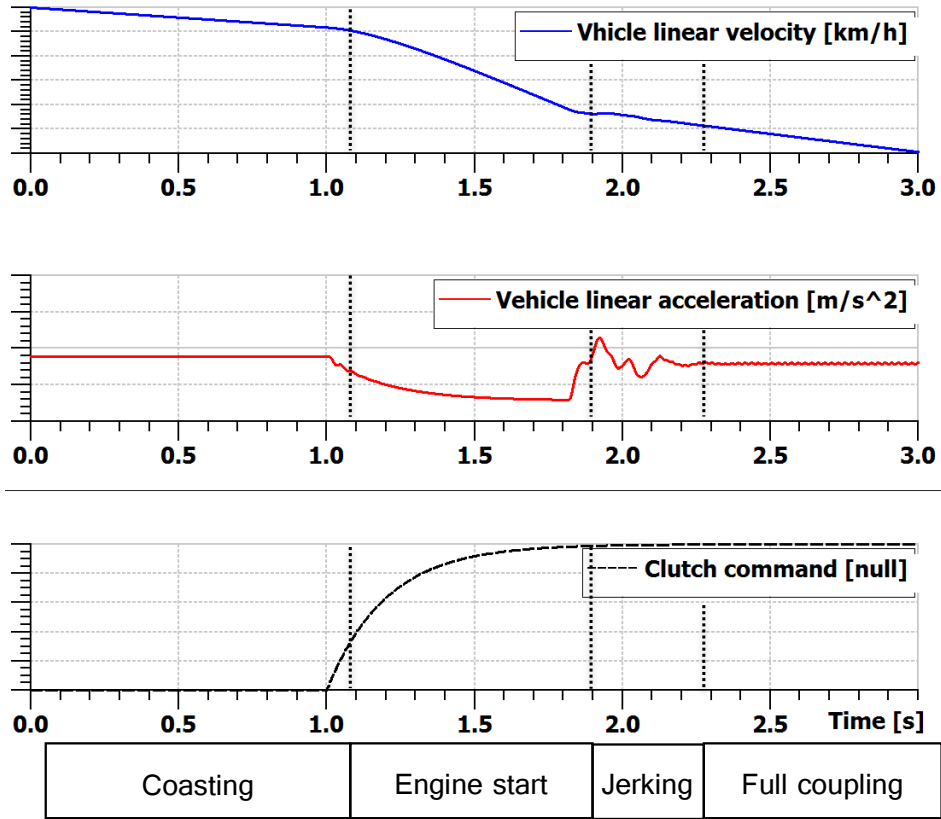


Figura 4.4: Vehicle velocity and acceleration during engine start via clutch at 50km/h 4th gear

able to correlate perception to physical measures. Today, procedures for the objective assessment of the subjective perception of the driver, as the corresponding evaluation method and formulas, are available on the market. Therefore, in order to evaluate drivability in a scientific way, AVL-Drive⁶ has been used to post-process simulation results of the drive-line model.

⁶Appendix B

4.2.1 Criteria & Requirements

Before starting any optimization of the control logic of clutch assisted start, it is important to set the main criteria for evaluation. Besides the clutch energy developed over such maneuver, the AVL Drive rating has been included: as AVL drive has no specific *clutch assisted engine start* maneuver implemented, then the regular AVL Drive maneuver *Tip in - After closed pedal* has been used.

Customer (internal, external)	Customer Expectation	Functional Measures for Quality [Units]		Target	Rationale (why?)	Evaluation Method
external	DQ – Tip-In delay & subcriteria	AVL Drive		>=7	Drivability	AVL Drive
subcriterion	Kick	CONTRIBUTION [%] Each single criterion contributes at the overall rating of the tip-in maneuver. If a single sub- criterion does not fulfill requirements, it prevents from reaching high ratings.			Drivability	AVL Drive
subcriterion	Initial Bump				Drivability	AVL Drive
subcriterion	Jerks				Drivability	AVL Drive
subcriterion	Response delay				Drivability	AVL Drive
subcriterion	Stumble				Drivability	AVL Drive
subcriterion	Torque build-up				Drivability	AVL Drive
subcriterion	Torque smoothness				Drivability	AVL Drive
subcriterion	Absolute torque				Drivability	AVL Drive
Internal	Clutch energy	Hill start identified as worst case		<Energy@ Hill Start	Durability	AmeSim

Figure 4.5: Criteria and requirements for evaluation of clutch assisted start.

Clutch energy By operating the clutch in slippage mode, a certain amount of energy is dissipated through the clutch system. The amount of energy dissipated through the clutch depends on the drag speed and the difference in speed between the two sides of the clutch.

$$\begin{aligned}
 \omega &= \frac{\omega_1 - \omega_2}{\Delta t} \\
 T_{drag} - T_{clutch} &= J \cdot \omega = \\
 T_{clutch} &= T_{drag} - J \cdot \omega = T_{drag} - J \cdot \frac{\omega_1 - \omega_2}{\Delta t}
 \end{aligned} \tag{4.14}$$

Where $J = J_{engine} + J_{DMF} + J_{clutch_cover}$, then energy can be calculated as:

$$E = T_{clutch} \cdot \frac{\omega_1 - \omega_2}{2} \Delta t \tag{4.15}$$

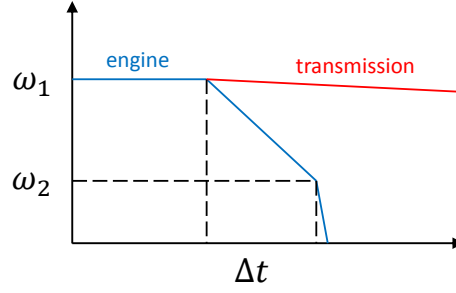


Figure 4.6: Difference in speed between the two sides of the clutch.

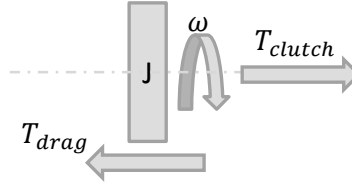


Figure 4.7: Clutch torque.

The energy generated over clutch assisted start must be lower than clutch energy generated over hill start, which represent the most critical condition for the clutch system.

Tip-In delay AVL Drive evaluates the *tip-in delay* of the vehicle by a weighted average of a set of sub-criteria, evaluating defined objective measures. Appendix ?? reports details of the tool.

Figure 4.6 reports the values for assessment for drivability. A rating of 7 is accepted.

4.2.2 Methodology

During the optimization of clutch control, two main task have been performed:

- *Evaluate applicability of Clutch Assisted Start* according to vehicle speed, gear engaged, accelerator pedal position⁷. Should Clutch Assisted Start

⁷ Accelerator pedal is the main interface between driver and vehicle: engine controller evaluates

Criterion	Percentage
Kick	$x/100$
Initial bump	$x/100$
Jerks	$x/100$
Response delay	$x/100$
Stumble	$x/100$
Torque build-up	$x/100$
Torque smoothness	$x/100$
Absolute torque	$x/100$
Overall Rating	100

Tabella 4.1: AVL Drive - Tip-in criteria weight list

AVL-DRIVE™ Driveability Assessment		
DR	Evaluation	Description
9 - 10	excellent	The driveability exceeds all customer's expectations
8 - 9	good	The driveability meets all customer's expectations
7 - 8	satisfying	The driveability meets most customer's expectations
6 - 7	acceptable	Driveability at basic level only, does not meet most customer's expectations
5 - 6	poor	Some customers complain about driveability
4 - 5	unacceptable	Most customers complain about the driveability
3 - 4	defective	All customers complain driving the vehicle
2 - 3	unsafe operation	Only limited or unsafe vehicle operation possible
1 - 2	no operation	Vehicle not operational

Figura 4.8: AVL Drive Drive™ *Drivabilityassessment*.

not be applicable, due to drivability requirements, either engine will be cranked via conventional starter or engine auto-stop will not be allowed.

- *Optimize the clutch torque T_c* transferred by the clutch to the engine in order to crank it.

The model so far developed in Chapter 3 will be used to run simulation of clutch assisted start in different conditions.

the torque, and therefore the vehicle acceleration, requested by the driver by means of the pedal position.

Input parameters It is important, then, to evaluate the input parameters of the model which defines the operating conditions of the vehicle:

- *Vehicle speed*, varying from 20 to 120 km/h ;
- *Gear engaged during sailing* varying from 2nd to 6th km/h;
- *Accelerator Pedal Position* (PPS) at next tip-in when exiting sailing 20% to 100%;
- *Clutch torque* (T_c) transferred via clutch;
- *Crank mode*: via starter (= 1) or clutch assisted start (= 2).

Output parameters The output signals of the drive-line model will then postprocessed via AVL Drive. Evaluation of clutch assisted start applicability will then perform on the following measures, according with main requirements identified:

- *Clutch Energy*;
- *Absolute torque*, sub-criterion of AVL Drive Tip-in rating;
- *Kick*, sub-criterion of AVL Drive Tip-in rating;
- *Initial bump*, sub-criterion of AVL Drive Tip-in rating;
- *Jerks*, sub-criterion of AVL Drive Tip-in rating;
- *Response delay*, sub-criterion of AVL Drive Tip-in rating;
- *Stumble*, sub-criterion of AVL Drive Tip-in rating;
- *Torque build-up*, sub-criterion of AVL Drive Tip-in rating;
- *Torque smoothness*, sub-criterion of AVL Drive Tip-in rating;
- *Overall rating* of tip-in in AVL Drive.

Collecting data for all different conditions by a full factorial combination of input parameters would require a significant number of simulation runs. To reduce the computational effort, a ‘Design of Experiment’⁸ would be the best fit, as it reduces the number of combination of input parameters to collect data. Figura4.9 reports the major steps of the test procedures for data collection.

⁸The DoE described in this section has been designed using ‘Kriging Tool’ available in MS Excel.

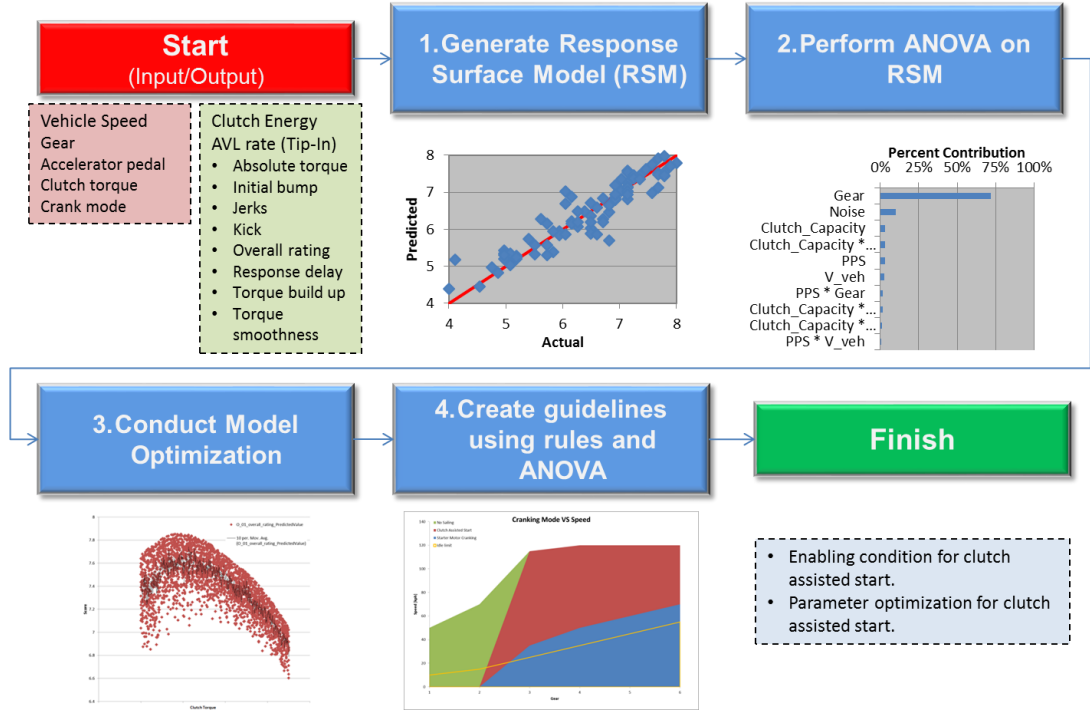


Figure 4.9: Test procedure & data collection.

Generation of test plan A space-filling Design of Experiments (DOE), so called a STOA DOE with Latin hypercube square approach (range limits only), is adopted, as range information are known for all input parameters. This parameter range information will be applied to the DOE design. The results should be a DOE test plan that does not violate physical constraints of the system during the simulation runs (i.e. low speed and high gear as in Figura4.10).

Given the n main input parameters in , then an appropriate test-plan, STOA DOE, has been generated: the minimum number of test point has been set to n^2 .

Response Surface Model (RSM) Once the simulation runs are performed and output data collected, a Response Surface Model has been created. A Response Surface Model (RSM) is a function which governs the input-to-output relationship associated with a CAE model. The Kriging method has been used to generate the Response Surface Model. Each output has its own Response Surface Model.

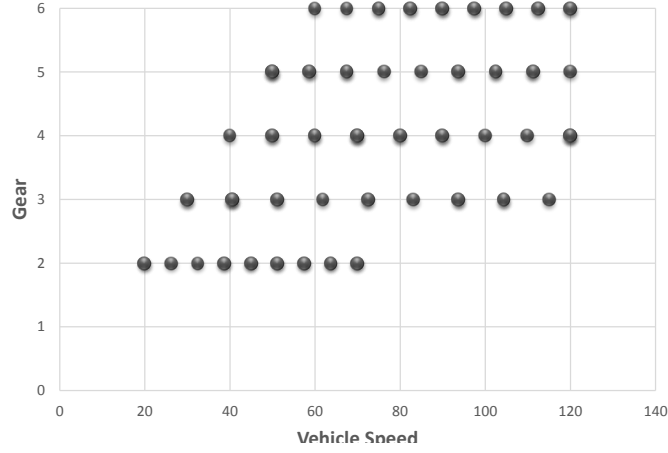


Figura 4.10: Generation of test-plan.

Analysis of Variations (ANOVA) The purpose of performing the ANOVA analysis is to identify the percent contributions of input variables for each corresponding output variables. If any input parameter used in the RSM has higher percent contributions, then this specific parameter should be treated seriously. Higher percent contribution means its influence on the performance is bigger. Thus one needs to pay more attention to such parameter when performance tuning is required later. The trends of output variables changing with tuning the input variable are provided by ANOVA analysis. Figura4.11 gives the percentage contribution of the input variables and interactions on the *Overall Rating of Tip-In*. These charts are generated for each response in the RSM, for each output parameter.

The main parameter influencing the overall rating appears the gear engaged, while the vehicle speed appears to have almost no influence on the rating as described in .

RSM optimization The optimization of the RSM model means finding values for each input parameter which allow to generate output within targets set. The first step in the optimization process is to generate mass solutions for entire domain of variations of parameters. By using the RSM generated for tip-in maneuver to exit a sailing event, it is possible to explore the entire test domain without running additional simulation point. By creating a STOA DOE with the infinite number of test runs n^∞ , a *virtual data-set* is created by predicting the response values with the RSM. Due to the nature of the STAO DOE design this will provide high resolution coverage of the entire test domain.

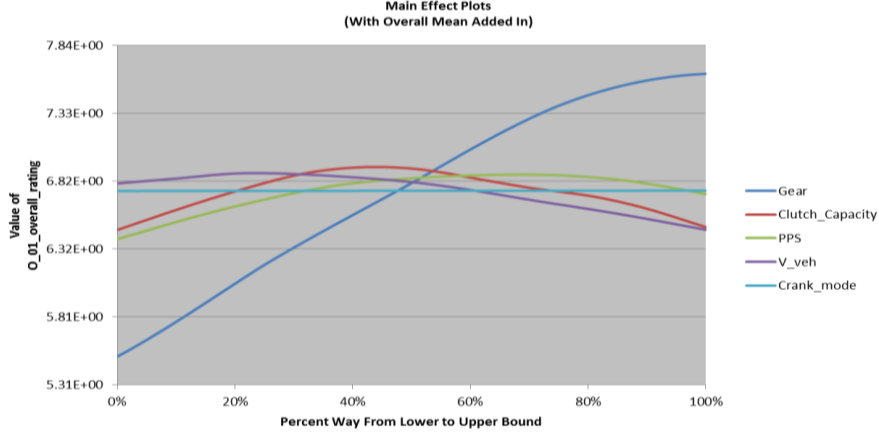


Figura 4.11: Percentage of contributions of each input parameter on the overall rating.

By applying opportune filtering of data⁹ and by selecting only simulation point with ‘clutch assisted start’¹⁰, an optimized clutch torque value T_c has been predicted for each vehicle conditions, defined by gear, speed and pedal position. The responses within the entire domain are filtered based on the targets determined in the 4.2.2.

Figura4.12 reports the optimized values of clutch torque for clutch assisted start to achieve the desired target on overall rating (≥ 7).

Such task allows to achieve the first goal of calibrating the clutch torque value.

Creating guidelines using rules and ANOVA In order to evaluate the range of applicability of clutch assisted start, the *virtual data-set* has been filtered according to defined target in order to evaluate range of applicability of clutch assisted start.

⁹MS Excel has been used to filter the *virtual data-set*.

¹⁰Crank mode equal to 2.

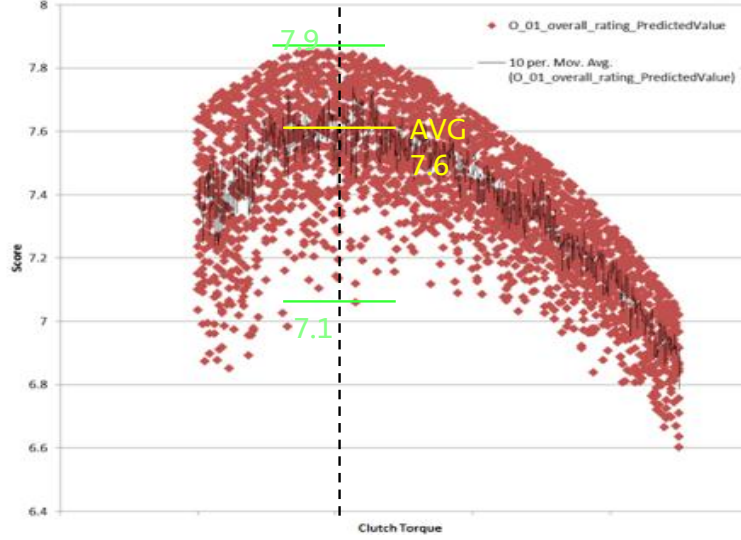


Figura 4.12: Optimization of clutch torque to achieve target overall rating for Tip-In in AVL Drive.

Guidelines have been created in order to understand when clutch assisted start could be enabled:

- Minimum *vehicle speed* to enable clutch assisted start per each gear, as shown in Figura4.13;
- Minimum *accelerator pedal position* to enable clutch assisted start per each gear, as shown in Figura4.14;

4.3 Results

The ANOVA 4.2.2 analysis has showed that the gear has the major influence on the overall rating of tip-in; such result could be explained mainly for two reasons:

- Equation 4.10 shows that an higher i_g leads to an higher deceleration \dot{v}_v , due to an higher value of lumped mass m_{vwt} . Therefore especially at low gears, higher vehicle deceleration are expected when coupling engine to the driveline;

- Drivers expect faster reaction at tip-in, lower response delay at lower gears than at higher ones.

Therefore, when looking at guidelines for applicability of clutch assisted start all conditions are referring to the gear engaged.

By evaluating Figura4.13, clutch assisted is allowed only at higher vehicle speed, as the vehicle has more kinetic energy, the energy required to crank the engine is less significant than at lower speed: in fact, reducing the kinetic energy would lead the vehicle to decelerate more at lower speed. At low speed, therefore, it is convenient to crank engine via starter, in order to affect jerking of the vehicle. Moreover, AVL Drive overall rating of tip-in shows that higher response delay are accepted at low speed.

Clutch assisted start, as per Figura4.14, is more effective at higher accelerator pedal position, mainly due to the fact that driver expects faster response of the system and can accept jerking of the vehicle. AVL Drive overall rating of tip-in proves such driver's perception.

Clutch Assisted Start is allowed only when both conditions (Minimum vehicle speed and minimum accelerator pedal position) are met.

An outcome of the analysis of Figura4.13 and Figura4.14 is an evaluation of when engine-off sailing is allowed according to tip-in delay. By evaluating the overall rating for tip-in for both crank modes (Starter and Clutch Assisted Start), the tip-in delay when exiting sailing is evaluated: if requirements on drivability are not met also when cranking via starter, then engine-off sailing is not allowed.

The clutch torque transferred via clutch assisted start must be optimized for the different gears. By looking at results in Figura4.12, the optimal value of clutch torque to improve the drivability of the vehicle is found by an opportune trade-off between two sub-criterion of overall rating of Tip-in:

- *jerks* would require a low value of clutch torque for a smooth crank of the engine in order to avoid oscillations of the driveline;
- *response delay* would require an high value of clutch torque in order to rev the engine up fastly.

The value of clutch torque can be considered stable for the different gears as shown in Figura4.15. An higher value of clutch torque, indeed, would lead to better results on the overall rating of tip-in at high accelerator pedal position and at high vehicle speed, where lower response delay have more influence on driver's perception than jerking.

As final step of result of the analysis, the clutch energy analysis shows that energy generated over clutch assisted start is fulfilling initial requirement. The

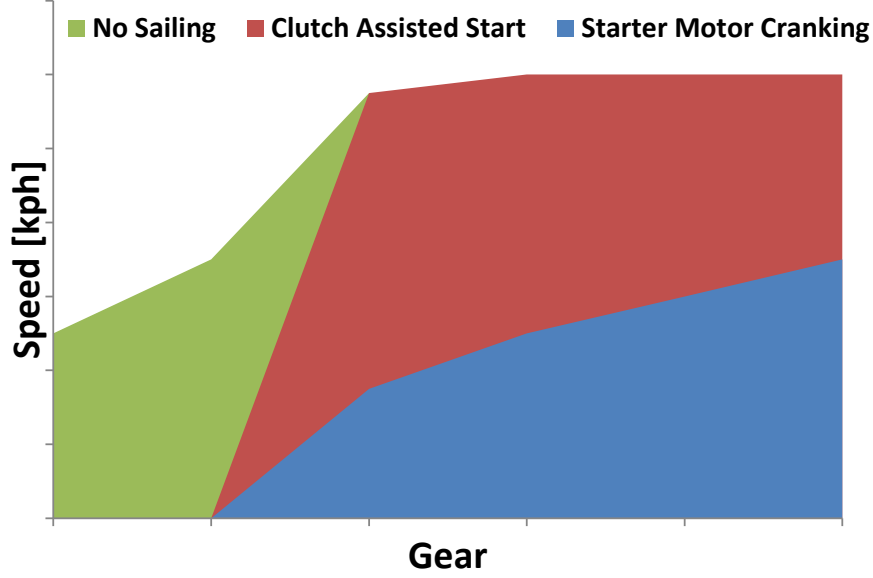


Figura 4.13: Applicability of clutch assisted start according to speed and gear.

energy developed to crank the engine depends on the value of clutch torque transferred when cranking the engine and on the energy generated when synchronizing engine and gearbox: as a matter of facts, as when cranking via starter, clutch torque is set to 0 (clutch open), the energy generated is lower than when cranking the engine via clutch. Moreover, due to the fact that the gear ratio i_g influence the lumped mass of the vehicle m_{vwt} by multiplying the inertia of the engine, more energy is generated at lower gears than at higher ones.

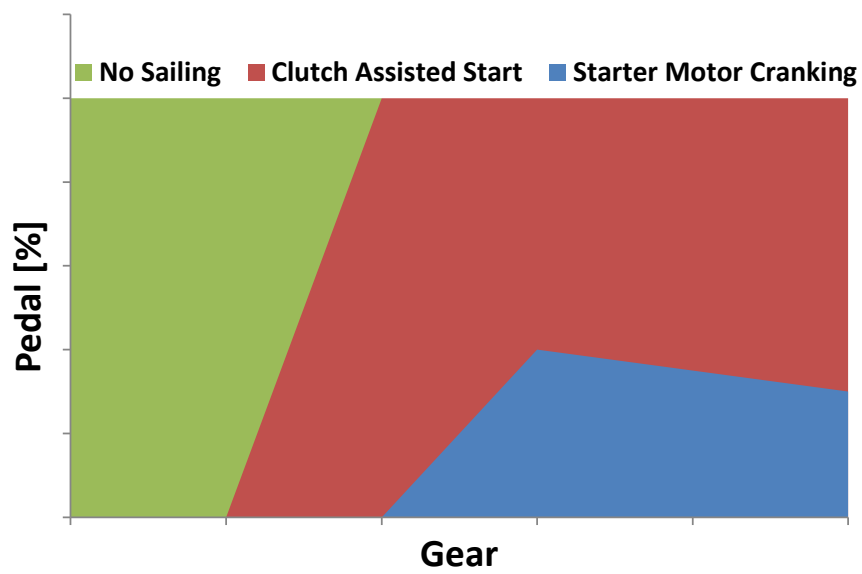


Figura 4.14: Applicability of clutch assisted start according to accelerator pedal position and gear.

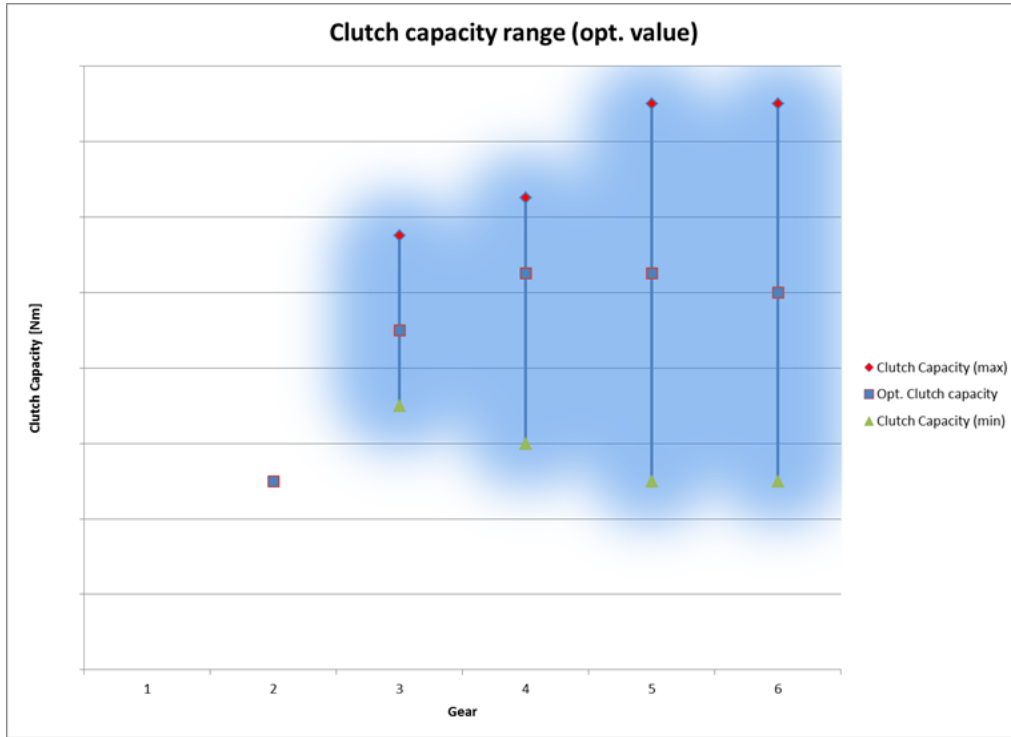


Figura 4.15: Optimal value of clutch torque and spread in different gear.

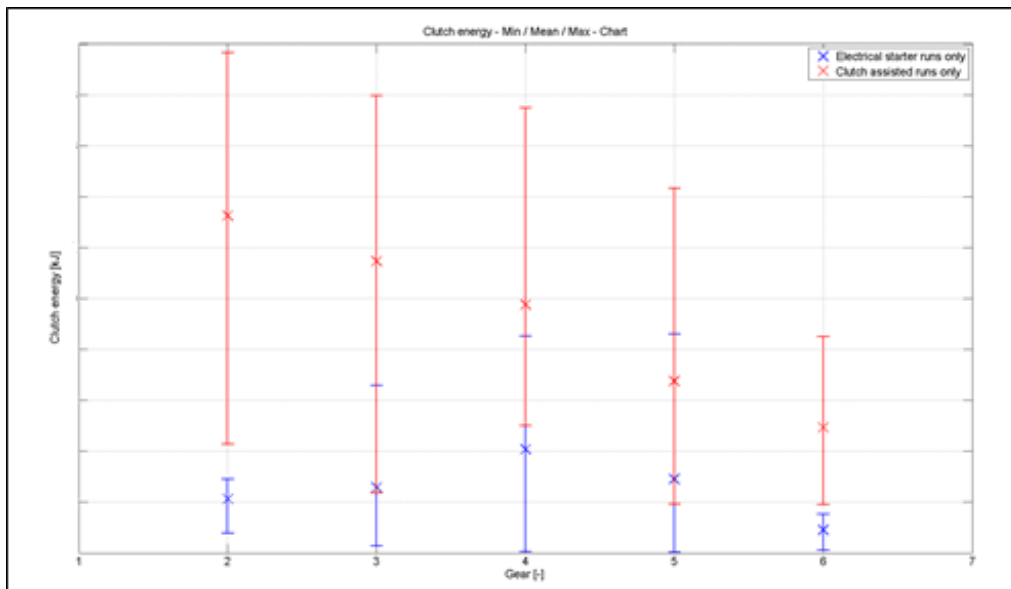


Figura 4.16: Clutch Energy over engine crank via starter (blue) and via clutch assisted start (red) generated over the different gears.

4.4 Conclusions

As the clutch assisted start achieves the main requirements set, ensuring an acceptable drivability of the system and generate an unfeasible value of clutch energy, it represents a viable solution to close the gap in system requirements when enabling S&S Sailing on powertrain.

By applying such control feature in powertrain equipped with an automated clutch, it is possible to overcome the two main issues: clutch assisted start reduces by 25% the engine crank time than when starting the engine via starter; then, by enabling engine crank via clutch, the durability of the starter would be ensured even if the number of engine crank over life time are increased.

Appendice A

In-cylinder pressure predictive model

In order to predict pressure development inside the cylinder during combustion a study based on thermodynamics equations was done. It is founded on a physic-based predictive engine combustion model.

A.1 Predictive Combustion Model

The combustion model has been developed in joined activity by Politecnico di Torino and GMPTE ATW Controls. It relies on the prediction of the heat released from fuel combustion (Figura

- *SOI* (start of injection)
- Quantity of injected fuel
- *ET* (injection time)

The net heat released in the chamber (Q_{ch}) is considered as a function of the heat released by the main and pilots fuel injected rate ($Q_{fuelmain}$ and $Q_{fuelpil}$) and four matching parameters achievable from experimental tests. These parameters are obtained minimizing mean square error between the Q_{ch} of predictive model and the one derived by pressure measurements from several bench tests. The thermodynamic behavior during combustion inside engine chambers is a complex topic and many factors contribute to the system dynamics. The main elements affecting the system that are considered are:

- Quantity of injected fuel
- Engine velocity

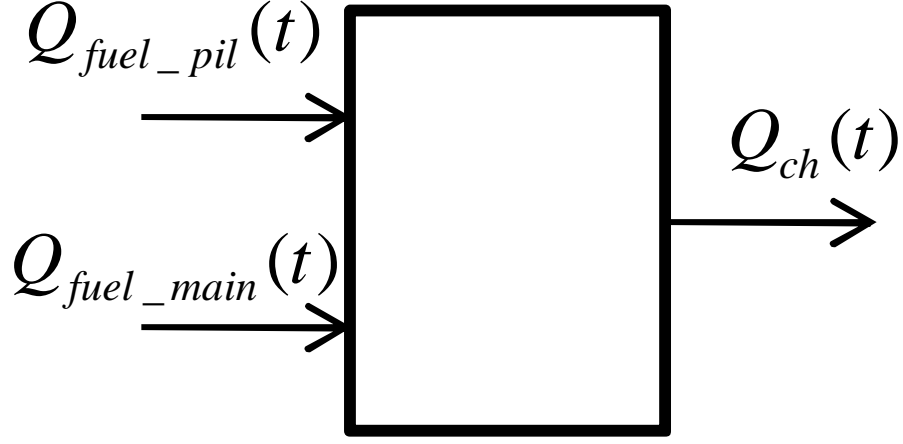


Figura A.1: Schematic of heat released from fuel combustion to the chamber.

- Load (*bmep*)
- O_2 (% of oxygen controlled by EGR valve)
- Temperature and pressure in manifold

Since this model was aimed to be used for engine start analysis, only low engine speeds were considered (1000, 1250, 1500 rpm) and furthermore the EGR valve should be off (combustion with $\approx 21\% O_2$) in nominal starting condition. The influence of temperature and pressure in manifold was neglected. Therefore several bench tests data were collected varying engine velocity and load. For each test condition, starting from the measured in-cylinder pressure and volume displaced by the piston in time, the effective HRC (Heat Released Cumulative) curve was calculated integrating the following expression (A.1):

$$\frac{dQ_n}{dt} = \frac{\gamma}{\gamma - 1} p \frac{dV}{dt} + \frac{1}{\gamma - 1} V \frac{dp}{dt} \quad (A.1)$$

For each test, the 4 matching parameters were found in order to minimize mean square error between Q_{ch}^{exact} derived from pressure measurement and Q_{ch} obtained by predictive model (FiguraA.3).

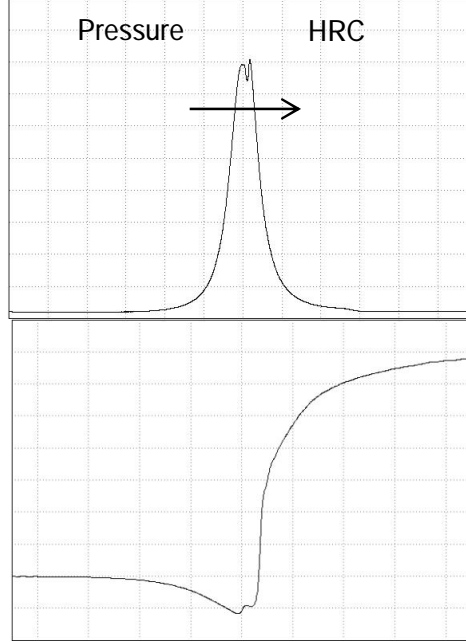


Figura A.2: In-cylinder pressure data and resulting HRC.

For each matching parameter identified it was found a polynomial model that expresses their relation to both engine speed and mean effective pressure. MATLAB surface fitting tool (sftool) was used for such purpose (FiguraA.4 shows an example):

Hence the combustion model requires only the desired engine velocity and brake torque (or *bme_p*) to identify, from fitting polynomial equations, the four required matching parameters. Knowing the fuel injected quantity, SOI and ET the final output of this predictive model is an HRC curve.

A.2 In-cylinder pressure generation

From the HRC data it is possible, considering the ideal gas law, to derive pressure values using the already considered expression (A.2). It is a first order differential equation in time domain and it was computed using Simulink. Knowing the instantaneous velocity, it was possible to switch from time domain to crankshaft angle domain. The volume variation with crankshaft angle can be computed from geometrical dimensions of engine components:

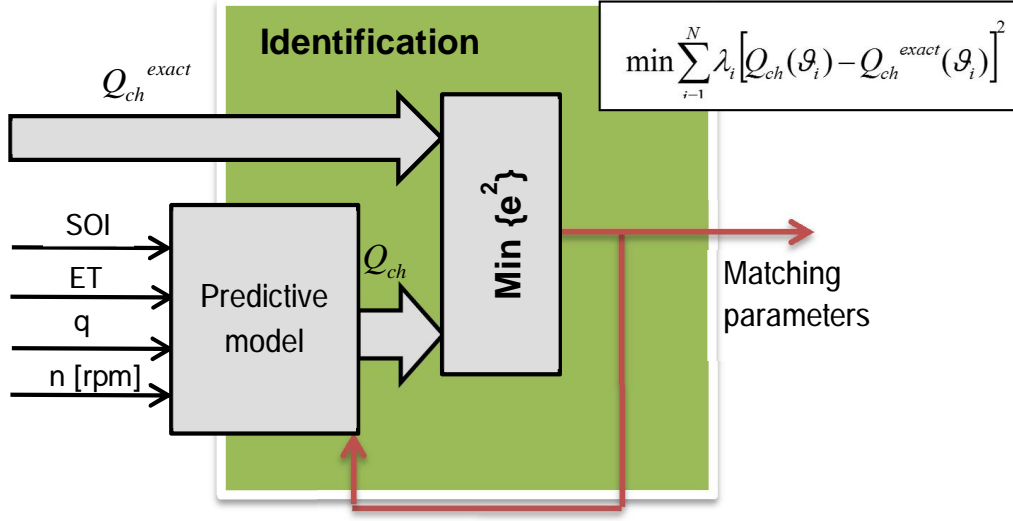


Figura A.3: Schematic of matching parameters identification method.

$$V(\theta) = R_c A_p \left[\frac{2}{CR - 1} + (1 - \cos \theta) + \left(\frac{L_c}{R_c} - \sqrt{\left(\frac{L_c}{R_c} \right)^2 - \sin^2 \theta} \right] \quad (\text{A.2})$$

The Simulink model provides in-cylinder pressure data from HRC for a complete engine cycle (720° crankshaft revolution) (FiguraA.5).

Considering the differential equation A.1, the resulting in-cylinder pressure simulated by the model is thus dependent not only on the combustion model HRC data, but also on γ , the isentropic expansion factor (or adiabatic index). It generally depends on the gas composition and on the temperature. For this study a constant value of γ is considered. Another important aspect for the pressure model is the behavior of intake and exhaust valves. Intake valve closure determines the starting point of the adiabatic compression stroke, while exhaust valve opening concludes the expansion stroke. From the valve diagram schematics (A.6), it was decided to consider the intake valves to be closed 35° after BDC (start of compression), and the exhaust valves to be opened 36.5° before next BDC.

The pressure inside the cylinders before intake valves closure was considered to be at atmospheric value (1.01325 bar) and also after exhaust valve opening the pressure drops at this value. The pumping losses (pressure drops) are not added

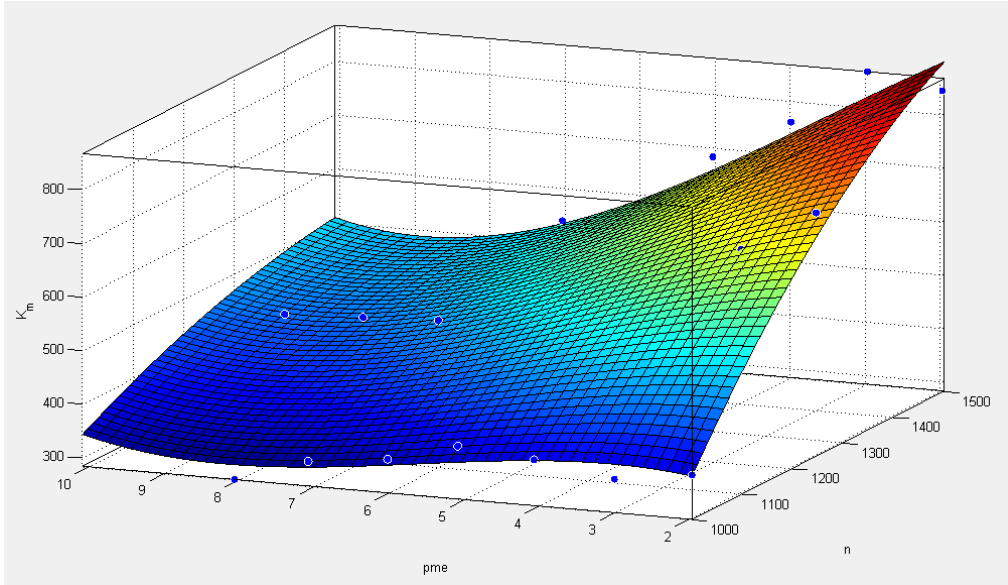


Figura A.4: Matching parameter as a function of both engine velocity and $bmep$.

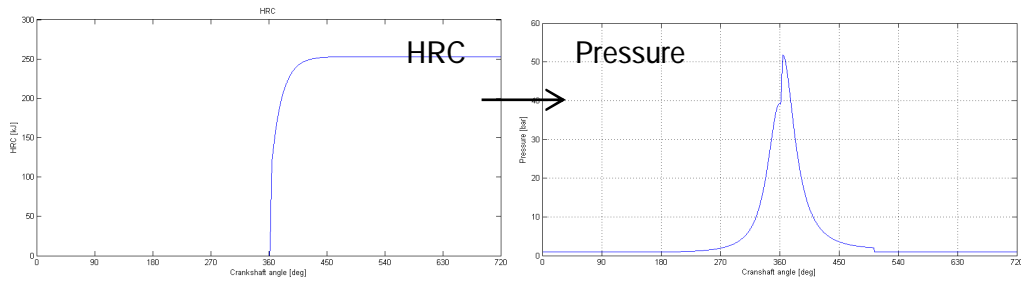


Figura A.5: HRC predicted by the combustion model and resulting pressure wave.

to the model since they are considered in the experimental friction map. In order to validate these assumptions an experimental pressure wave is compared to a simulated one in the case of motored engine, that is a compression-expansion of the air inside the cylinder without injection and combustion ($dQ_{ch} = 0$) (FiguraA.7).

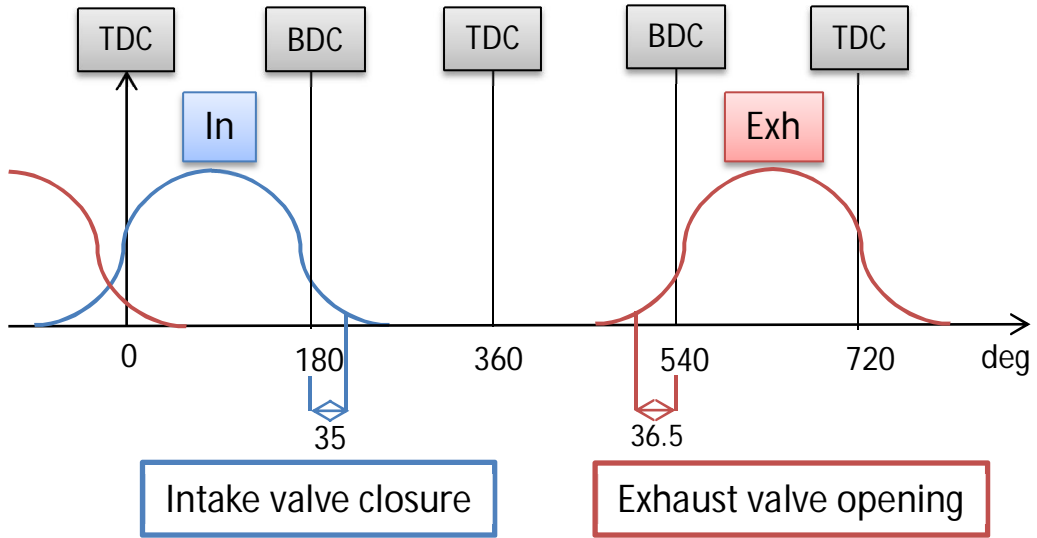


Figura A.6: Schematic of intake and exhaust valves diagram with opening and closure angle.

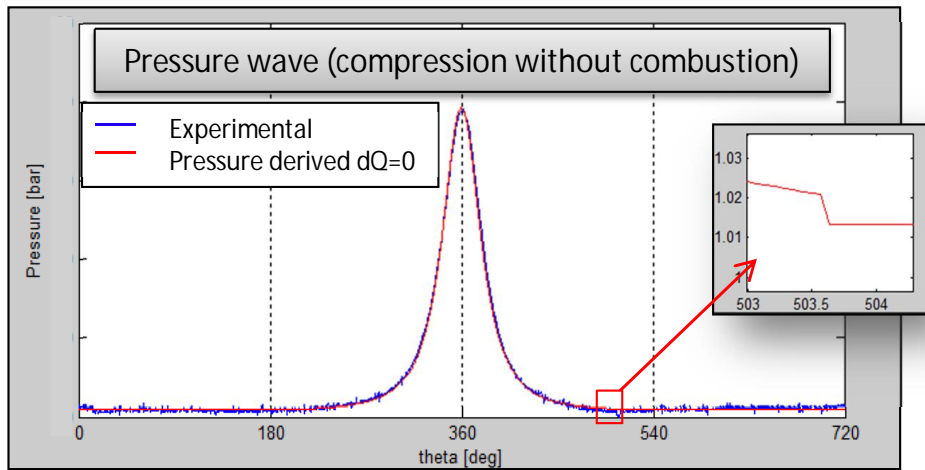


Figura A.7: In-cylinder pressure for motored engine (0 fuel).

A.3 Multi-cylinder pressure model

Since the computation of in-cylinder pressure is based on crank angle domain, in order to have pressure values for all 4 cylinders, it is sufficient to consider a

shift of 180° of the crankshaft angle for each cylinder in their firing order. The crankshaft angle is the derivative in time of the angular velocity. Therefore, having the instantaneous velocity, a multi-cylinder model is set up, able to generate pressure data for each cylinder, which phase is based on crankshaft position. In other words, considering the general angular variation of the system $\theta(t)$, for each cylinder the phase shift can be expressed as: $\theta_i(t) = \theta(t) + 180 * (i - 1)$ where i is the firing order position of the considered cylinder ($i = 1$ for cylinder 1, $i = 4$ for cylinder 2, $i = 2$ for cylinder 3, $i = 3$ for cylinder 4). The model calculates the pressure from the differential equation (A.1) independently for each cylinder, having in input the crankshaft angle variation in time $\theta_i(t)$. An example for a complete engine cycle (720°) for all the 4 cylinders is shown (Figura A.8) in the case of motored engine (no combustion, $dQ = 0$).

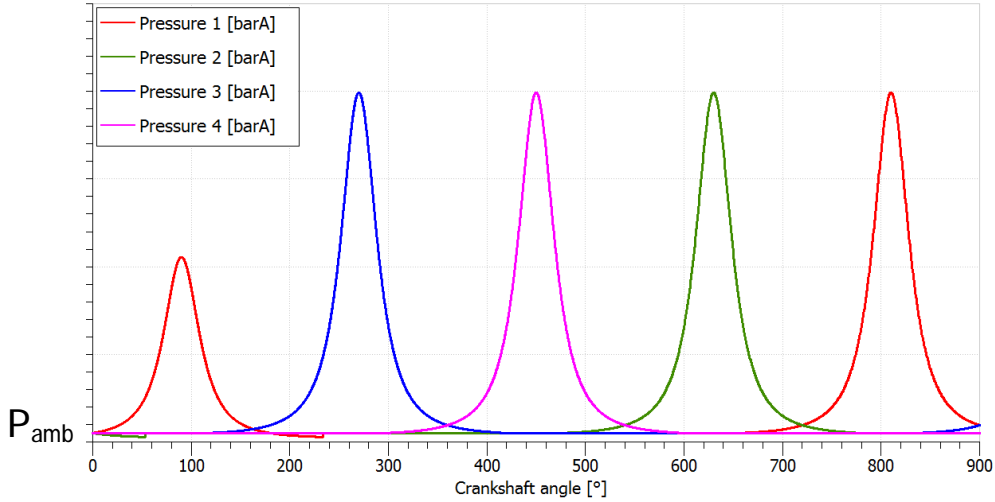


Figura A.8: In-cylinder predicted pressure for the 4 cylinders.

A.4 Co-simulation between AMESim & MATLAB/Simulink

In order to implement the pressure model in the AMESim engine model, a co-simulation between MATLAB/Simulink and AMESim is arranged. Essentially the Simulink model can be converted into an AMESim block compiled in C++

with a fixed time step approach. The block generated is shown in FiguraA.9. The inputs to the Simulink block are provided by AMESim simulation and the pressure data output for each cylinder are generated instant by instant depending on the system conditions.

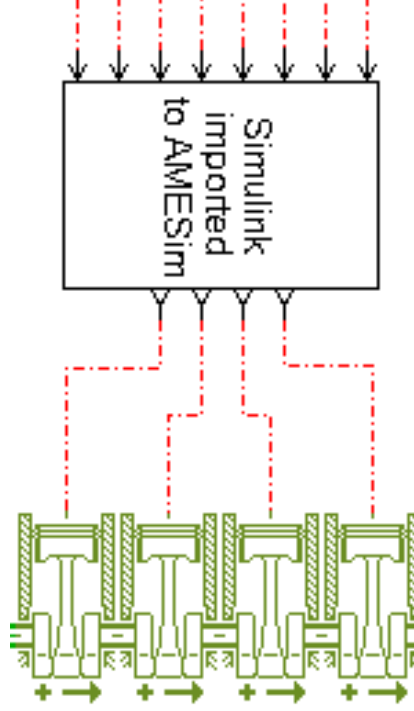


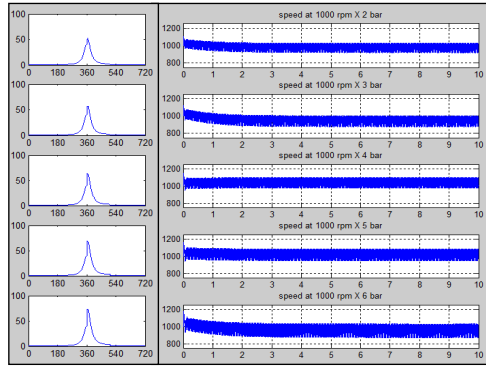
Figura A.9: AMESim model with Simulink pressure block.

The inputs are:

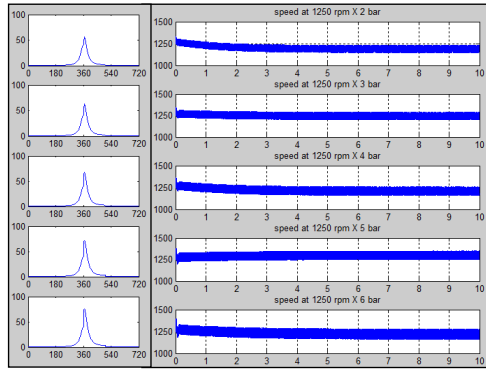
- crankshaft angle with phase shift for each cylinder;
- crankshaft velocity;
- load and friction torque.

The crankshaft angle variation is essential for the generation of the pressure wave through the differential equation (3.1). While the engine speed and load (plus friction) torque are needed to obtain the matching parameters and quantity of fuel injected (from fuel map) necessary to the combustion model. Accordingly, from the pressure data generated, the AMESim model calculates

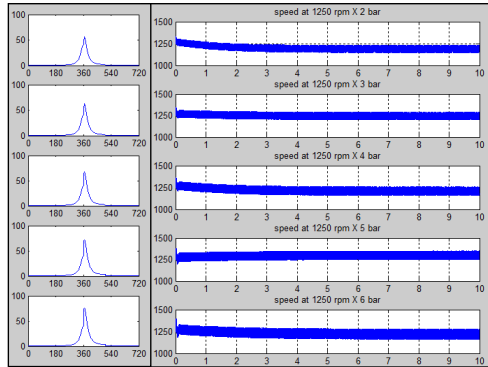
the resulting torque. In order to validate the complete system, the simulated engine speed should reach an equilibrium state at a required value. This means that the pressure wave, calculated by the combustion model, should generate a resulting torque, from piston to crankshaft, able to balance engine frictions, inertias and imposed resistive load, keeping the engine speed at the desired value. The load (brake torque) is added to the model as an opposing torque operating on the secondary mass of the flywheel. While the friction curve used was experimentally acquired by motoring the engine for different speeds, since with this procedure pumping losses are included (see frictions description section). Simulations were run for different engine speeds and load conditions. The results for crankshaft velocities at 1000, 1250, 1500 rpm and bmep of 2, 3, 4, 5, 6 bar are plotted in the FiguraA.10.



(a) 1000 rpm



(b) 1250 rpm



(c) 1500 rpm

Figura A.10: Simulated engine speed resulting from predicted in-cylinder pressure

Appendice B

AVL-Drive (21)

The AVL-DRIVE system is designed for objective assessment and quality control of drivability based on human experience. The intent is to set procedures for the objective assessment of the subjective perception of the driver. AVL-DRIVE uses different vehicle information, data and parameters, such as accelerations, engine data, vehicle speed, and pedal position. These input quantities are collected in specific maneuvers.

B.1 System Overview

The AVL-DRIVE system is designed for objective assessment and quality control of drivability based on human experience. Procedures for the objective assessment of the subjective perception of the driver have been used to define the evaluation method and formulas. Vehicle data from sensors are correlated at the same time at subjective ratings of a range of drivers has been collected by a generic algorithm. For each single operating mode, maneuvers.

AVL-DRIVE use different sensors and CAN bus information to capture the most significant data and vehicle parameters, such as longitudinal acceleration, engine speed, vehicle speed, and pedal position. These input quantities are collected by the DMU2 (DRIVE Main Unit 2, located in the car boot) and passed on to a PC (Notebook, located at the passenger seat) for further analysis.

In FiguraB.1, sensors 1, 4, 5 and 6 capture the influence on the driver.

The AVL-DRIVE system relates data for different vehicle classes (Small, Medium, Large, Compact, Luxury, Sportive, SUV, Pick-up Truck, Light / Heavy duty truck, and Tractors) and the following transmission variants:

- MT

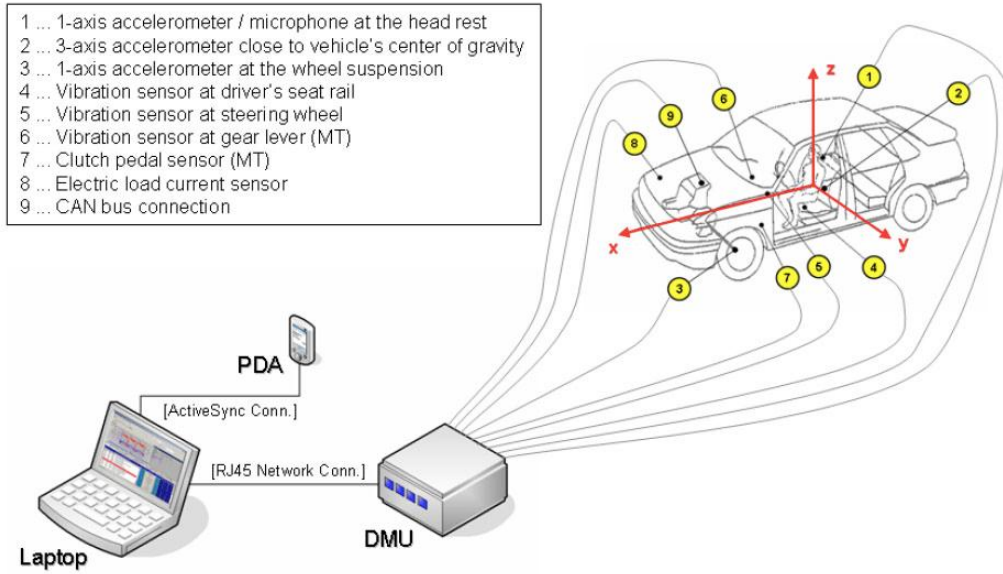


Figura B.1: The components of AVL-DRIVE system.

- MTA
- AT
- DCT
- CVT
- HEV
- EV

In the AMT transmission has been considered in order to reflect typical behavior at tip-in. As a matter of facts, due to the novelty of the maneuver investigated in this project, no previous data are available for benchmark. More than 500 individual criteria (i.e. Kick, Surge, Engine speed fluctuation, Response delay, etc.) are identified for several driving modes (i.e. Drive away, Acceleration, Gearshift, Tip-in, etc.). The relevant parameters for defined criteria of all detected driving modes are measured, calculated, weighted and recorded. The AVL-DRIVE system delivers objective ratings for drivability quality and vehicle character and - combined with an automatic classification of similar driving modes - enables a very quick vehicle analysis. The drivability itself is assessed

at criteria level by means of a Drive Rating (DR) from 1 to 10 according to FiguraB.2.

AVL-DRIVE™ Driveability Assessment		
DR	Evaluation	Description
9 - 10	excellent	The driveability exceeds all customer's expectations
8 - 9	good	The driveability meets all customer's expectations
7 - 8	satisfying	The driveability meets most customer's expectations
6 - 7	acceptable	Driveability at basic level only, does not meet most customer's expectations
5 - 6	poor	Some customers complain about driveability
4 - 5	unacceptable	Most customers complain about the driveability
3 - 4	defective	All customers complain driving the vehicle
2 - 3	unsafe operation	Only limited or unsafe vehicle operation possible
1 - 2	no operation	Vehicle not operational

Figura B.2: Table for drivability rating in AVL-Drive.

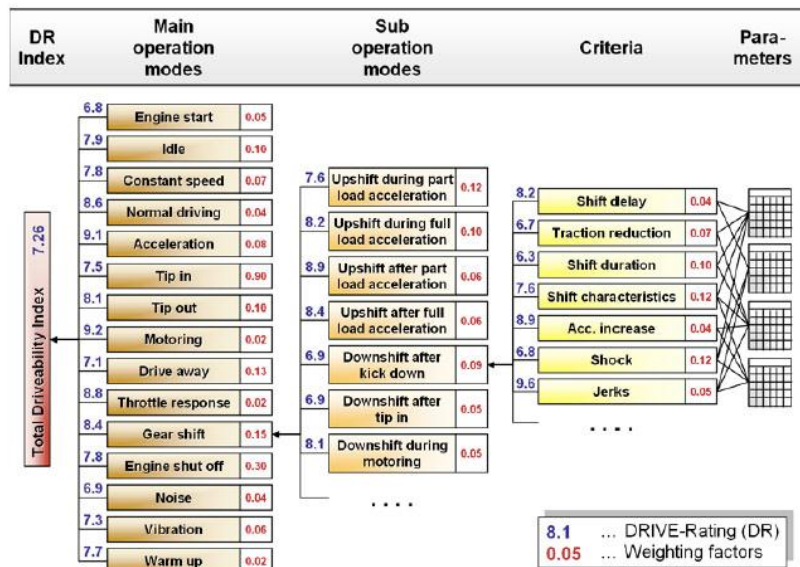


Figura B.3: Tree of main operation modes, sub operation modes and criteria.

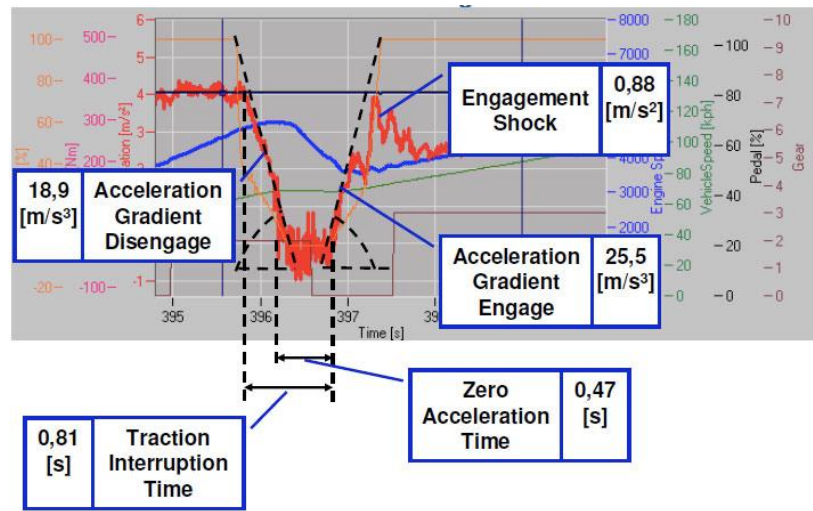


Figura B.4: Example of parameter calculation for single event.

FiguraB.3 reports an example of hierarchy of how main operation modes are evaluated via predefined criteria. FiguraB.4 reports as an example how different parameters are calculated for a single event of a gearshift such as, the acceleration gradient for disengagement of the gear, traction interrupt time, zero acceleration time, acceleration gradient on engagement of the gear and the engagement shock.

Appendice C

ACRONYMS

AHSS	Advanced High Strength Steel
AT	Automatic Transmission
BAS	Belt Alternator Starter
BDC	Bottom Dead Center
BIW	Body-In-White
COG	Center of Gravity
CVT	continuously variable transmission
DCT	Dual Clutch Transmission
DFCO	Deceleration Fuel Cut-Off
DMF	Dual Mass Flywheel
DoH	Degree of Hybridization
EGR	Exhaust Gas Recirculation
EM	Electric Machine
EREV	Electric Range Extender Vehicle
ET	Energizing Time
EV	Electric Vehicle
FAS	Flywheel Alternator Starter
FE	Fuel Economy
FFT	Fast Fourier Transform
HEV	Hybrid Electric Vehicle
HOS	Hybrid Operating Strategy

HRC	Heat release cumulative
ICE	Internal Combustion Engine
IWC	Inertia Weight Class
LQ	Linear Quadratic
MGU	Motor Generator Unit
MT	Manual Transmissions
MTA	Automated Manual Transmission
NEDC	New European Driving Cycle
OEM	Original Equipment Manufacturer
PHEV	Plug-in Hybrid Electric Vehicle
S&S	Start/Stop, Engine Start/Stop-System
SOC	State Of Charge
SOI	Start of Injection
SQP	Sequential quadratic programming
TC	Turbo charged internal combustion engine
TDC	Top Dead Center
WLTP	World-wide Light-duty Test Procedure

Bibliography

- [1] 2008, SAE J1715 *Information Report: Hybrid Electric Vehicle (HEV) & Electric Vehicle (EV) Terminology*, SAE technical paper series, Detroit, MI.
- [2] Miller, Holmes, Conlon, Savagian. 2011, *The GM Voltec 2ET50 Multi-Mode Electric Transaxle*, SAE 2011 – 01 – 0887.
- [3] Morra, Spessa, Ciaravino, Vassallo. 2012, *Analysis of various operating strategies for a parallel-hybrid diesel powertrain with a belt alternator starter*, SAE World congress and exhibition, SAE Paper No. 2012 – 01 – 1008.
- [4] *ECE Regulation No. 101*.
- [5] Brunetti, Cisternino, Belingardi. 2012, *Early design methods for an HEV - Optimizing HEV vehicle design to achieve CO2 targets*, ISEV Conference, Warsaw.
- [6] Fedorov, Valerii, Hackl, Pete. 1997, *Model-Oriented Design of Experiments. Lecture Notes in Statistics.*, Springer-Verlag.
- [7] Montazeri-Gh, Poursamad, Ghalichi. 2006, *Application of genetic algorithm for optimization of control strategy in parallel hybrid electric vehicles*, Journal of The Franklin Institute 343 (2006), 420 – 435.
- [8] Millo, Badami, Ferraro, Rolando. 2009, *Different Hybrid Powertrain Solutions for European Diesel passenger cars*, SAE Paper No. 2009 – 24 – 0064.
- [9] MathWorks *MATLAB - The Language Of Technical Computing*, www.mathworks.com/products/matlab.
- [10] Miller, Rizzoni, Li. 1999 *Simulation-based hybrid-electric vehicle design search*, SAEpaper 1999 – 01 – 1150.

- [11] Grebe, Nitz. 2011, *Electrification of General Motors Vehicles A portfolio of solutions*, International Vienna Motor Symposium.
- [12] Ricardo report to GM Workshop - Passenger Car CO₂ (2012) *The route to 95g/km by 2020 Technology & Trends*.
- [13] Smith, Lippert. 2007, *The Drive For Energy Diversity and sustainability: The Impact of transportation Fuels and Propulsion System portfolios*, Germany.
- [14] Weber, 2003, *Vehicle System Modeling in the Automotive Industry*, AROERC Engine Modeling Symposium, University of Wisconsin-Madison.
- [15] Atluri, Weber. 2008, *Fuel Economy Potential of Advanced Powertrain Concepts*, PSR-187.
- [16] Steven. 2014, *Homologation test cycles worldwide - Status of the WLTP*, IEA, 13th April
<http://www.iea.org/media/workshops/2013/gfeilabelling/07.08.Homologationtestcyclesworldwide.pdf>
- [17] Mueller, Strauss, Tumback, Goh, Christ. 2011, *Next Generation Engine Start/Stop Systems: Free-Wheeling*, SAE, 2011-01-0712
- [18] Lo, Luan, Tate, Zarger. 2006, *A Simulation Model for the Saturn VUE Green Line Hybrid Vehicle*, SAE, 2006-01-0441
- [19] Smith, Bucknor, Yang, He. 2011, *Controls Development for Clutch-Assisted Engine Starts in a Parallel Hybrid Electric Vehicle*, SAE, 2011-01-0870
- [20] Vasca, Iannelli, Senatore, Taglialatela Scafati. 2008, *Modeling Torque Transmissibility for Automotive Dry Clutch Engagement* American Control Conference, WeA09.3
- [21] Nybacka, Holmlund, Danner. 2009, *AVL-DRIVE pre-study report*, Lulea University of Technology, SWEDEN, ISBN: 978 – 91 – 7439 – 008 – 7
- [22] 2008, *AVL-DRIVE product guide*, AVL List, Graz
- [23] Dolcini, Canudas-de-Wit, Bechart. 2010, *Dry Clutch Control for Automotive Applications*, Springer

- [24] Jiang, Chen, Zhang, Chen. 2009, *Multi-domain Modeling and Simulation of Clutch Actuation System Based on Modelica*, SAE International Journal Engines 2(1):1125-1131
- [25] Fasana, Marchesiello. 2006, *Meccanica delle vibrazioni*, CLUT
- [26] Mustafaj. 2013, *Modeling of vehicle driveline enabling clutch assisted engine start*, Politecnico di Torino-GMPT-E, 2013

Elenco delle figure

1.1	Layout of the considered hybrid powertrain	2
1.2	Hybrid powertrain layout according to the type of parallel HEV.	4
1.3	The amount of electrification at each degree of hybridization.	5
1.4	Impact on costs of technologies for mass reduction of BIW.	8
1.5	Impact of vehicle mass on energy, power required over NEDC homologation cycle.	9
1.6	Index of performance: impact of engine displacement.	10
1.7	Cost increase according to vehicle design parameters.	12
1.8	4D projection of experiments for the design.	12
1.9	Compare of predicted values and observed values of CO ₂	13
1.10	The optimization tool interface.	15
1.11	Available technical solution to achieve fuel consumption reduction - courtesy of Ricardo: GM workshop May 2012.	16
1.12	Impact of battery size on CO ₂ figures.	16
1.13	Impact of battery size on Pure EV driving.. . . .	17
1.14	Impact of battery size on vehicle mass.	18
1.15	Technology road map for electrification of diesel engines.	19
2.1	a) Engine Stop at vehicle in motion, b) Distance covered by vehicle with std S&S control strategy and vehicle adopting sailing during coasting.	22
2.2	Speed (a), acceleration (b) profiles of NEDC and WLTP	24
2.3	Engine fmep for different sizes of conventional light duty turbocharged diesels.	24
2.4	Fuel economy opportunity during idle phases over NEDC	25
2.5	Analysis of energy spent over cycle to propel the vehicle, motor the engine, charge the electrical system.	26
2.6	Coasting distance covered by a mid-sized vehicle in different gears and by rolling in neutral.	26
2.7	Sailing opportunity on vehicle	28
2.8	Power request over mid-segment of WLTP	30

2.9	Sailing events over WLTP	30
2.10	Fuel Economy scenario of Stop & Start technology over NEDC and WLTP	31
3.1	The AMESim model of the powertrain and driveline	35
3.2	Starting system schematic	36
3.3	Engine and starter motor modeling in AMESim	37
3.4	Starter motor AMESim modeling	38
3.5	Starter motor characteristic curve: Torque vs. Speed	39
3.6	Starter motor control system	40
3.7	Schematic representation of Dual Mass Flywheel	41
3.8	AMESim model of DMF.	41
3.9	DMF fluctuation reduction schematic.	42
3.10	Comparison between crankshaft velocity and secondary mass velocity.	42
3.11	Frequency domain of DMF compared to a torsional absorber clutch disk.	43
3.12	a)3D schematic of two-stage spring/damper system; b)Characteristic torque curve of the DMF	44
3.13	Simulated characteristic torque curve of DMF	44
3.14	Torque applied to DMF with an increasing and decreasing ramp function	45
3.15	Response of DMF to the torque applied: velocity difference of the two masses	46
3.16	Bode diagram of DMF in 1st stage	47
3.17	Bode diagram of DMF in 2nd stage	47
3.18	Resonance of DMF in 1st stage as a function of engine velocity	48
3.19	Velocities of DMF primary and secondary mass during engine starting phase	48
3.20	Engine modeling in AMESim.	49
3.21	Piston, connecting-rod and crank throw assembly schematic.	50
3.22	Friction model as a function of relative speed with stiction effect.	53
3.23	Friction map from the two methods: motoring and considering pumping losses; work integral over the combustion cycle not considering pumping losses.	54
3.24	In-cylinder pressure during engine motoring vs. crankshaft angle.	55
3.25	In-cylinder pressure during engine starting phase vs. crankshaft angle.	56
3.26	Engine cranking velocity with ideal gear meshing.	57
3.27	Engine cranking velocity with stiffness and backlash between gears.	58
3.28	Simulation of engine velocity during starting.	58
3.29	Schematic overview of powertrain.	60
3.30	Powertrain simplified model.	60

3.31	(a) Wheels velocity and engine velocity at 50 km/h in 4 th gear. (b) Torque on wheels and engine torque in 4 th gear.	62
3.32	Transmission modeling in AMESim.	62
3.33	Clutch system schematic.	63
3.34	(a) Coulomb friction model. (b) Tanh friction model.	65
3.35	Clutch system schematic.	66
3.36	Transmission modeling in AMESim.	67
3.37	Vehicle velocity trend for a coast-down test simulation with 0 road inclination.	69
3.38	Transmission modeling in AMESim with indicated torsional stiffnesses.	70
3.39	Vibrational modes of the transmission for gear 1 st to 3 rd	72
3.40	Vibrational modes of the transmission for gear 4 th to 6 th	73
3.41	Fast Fourier transform of engine velocity at idle.	74
3.42	Vibrational modes of the vehicle drive-line for gear 1 st to 2 nd	76
3.43	Vibrational modes of the vehicle drive-line for gear 3 rd to 4 th	77
3.44	Vibrational modes of the vehicle drive-line for gear 5 th to 6 th	78
3.45	Vibration of vehicle acceleration caused by matching tires resonant frequencies.	79
4.1	Basic explanation of clutch assisted start operation at tip-in.	83
4.2	Command force profile for LQ controller.	87
4.3	Torque transmitted T_c vs. throwout clutch position: (a, c) nominal characteristic, (b, d) characteristic: concave, (a,b) no wear, (c, d) in the presence of wear.(20)	88
4.4	Vehicle velocity and acceleration during engine start via clutch at 50km/h 4 th gear	89
4.5	Criteria and requirements for evaluation of clutch assisted start.	90
4.6	Difference in speed between the two sides of the clutch.	91
4.7	Clutch torque.	91
4.8	AVL Drive Drive TM Drivabilityassessment.	92
4.9	Test procedure & data collection.	94
4.10	Generation of test-plan.	95
4.11	Percentage of contributions of each input parameter on the overall rating.	96
4.12	Optimization of clutch torque to achieve target overall rating for Tip-In in AVL Drive.	97
4.13	Applicability of clutch assisted start according to speed and gear.	99
4.14	Applicability of clutch assisted start according to accelerator pedal position and gear.	100
4.15	Optimal value of clutch torque and spread in different gear.	101

4.16	Clutch Energy over engine crank via starter (blue) and via clutch assisted start (red) generated over the different gears.	101
A.1	Schematic of heat released from fuel combustion to the chamber. . . .	104
A.2	In-cylinder pressure data and resulting HRC.	105
A.3	Schematic of matching parameters identification method.	106
A.4	Matching parameter as a function of both engine velocity and <i>bmep</i> . .	107
A.5	HRC predicted by the combustion model and resulting pressure wave.	107
A.6	Schematic of intake and exhaust valves diagram with opening and closure angle.	108
A.7	In-cylinder pressure for motored engine (0 fuel).	108
A.8	In-cylinder predicted pressure for the 4 cylinders.	109
A.9	AMESim model with Simulink pressure block.	110
A.10	Simulated engine speed resulting from predicted in-cylinder pressure .	112
B.1	The components of AVL-DRIVE system.	114
B.2	Table for drivability rating in AVL-Drive.	115
B.3	Tree of main operation modes, sub operation modes and criteria. . . .	115
B.4	Example of parameter calculation for single event.	116

Elenco delle tabelle

1.1	The HEV powertrain layout	4
1.2	Attributes of Electrical Vehicles (1)	4
1.3	Energy content, usable SOC range of batteries according to the degree of hybridization of the powertrain	6
1.4	Vehicle segmentation	6
1.5	Main data of ICE focus of the analysis	7
1.6	Architecture 0 for balanced performance.	10
1.7	The functionality index.	11
1.8	DoE model results.	13
2.1	Key parameters of the NEDC, WLTP	23
2.2	Fuel economy figures of idle sailing vs. S&S sailing	31
4.1	AVL Drive - Tip-in criteria weight list	92